

The Surface Chemistry of Thin Lithium Metal Electrodes in Lithium-Sulfur Cells

Ming-Tao Lee,^{*[a]} Haidong Liu,^[a] and Daniel Brandell^{*[a]}

In this work, we explore the surface chemistry of Li metal electrodes used in Li–S batteries when employing a very thin (30 µm) lithium metal foil. The foil thickness is instrumental for achieving a balanced cell with optimal energy density, but previous work has largely neglected how the change to thinner anodes will influence the critical surface phenomena in the cell. X-ray photoelectron spectroscopy (XPS) was used as the main characterisation tool to follow the evolution of the solid electrolyte interphase (SEI) layer on the Li electrode, comple-

mented by scanning electron microscopy. Based on the XPS analyses, the premature capacity fading observed for the cell with thin Li metal electrode could be ascribed to changes in the composition of the surface layer on the Li electrode, due to that the resulting rougher surface more rapidly consume the LiNO₃ electrolyte additive. This highlights that mitigating the degradation mechanisms at the Li metal surface is of large importance when the Li electrode is scaled down for better cell balancing in Li–S cells.

1. Introduction

When facing the many global challenges concerning energy production, energy storage, and overall environmental impact from the energy sector, the lithium-sulfur (Li–S) battery can play an important role in the future energy system. Due to its attractive properties of high theoretical capacity and low cost, it is considered a very promising rechargeable battery chemistry. Sulfur is abundant, generally non-toxic and environmentally friendly. It combines a high theoretical capacity (1672 mAh g⁻¹) with a relatively low theoretical voltage of 2.24 V vs. Li⁺/Li, but still provides a very competitive gravimetric energy density (2600 Wh kg⁻¹) for a positive electrode material. Lithium metal likewise has a very high theoretical specific capacity (3860 mAh g⁻¹), and the lowest electrochemical potential of all elements. This constitutes the background to the substantial interest in Li–S batteries in recent years, where companies such as OXIS Energy^[1] and Sion Power Corporation^[2] have delivered cells with energy densities as high as 450 Wh kg⁻¹.

However, there are still many scientific and technical challenges which plague the Li–S batteries and need to be improved, not least high self-discharge, poor capacity retention and short cycle life. The two primary problems that limit the

development of Li–S batteries are the parasitic polysulfide shuttle^[3] and the instability of the lithium metal negative electrode, causing dendrite formation.^[4] The polysulfide shuttle occurs through spontaneous reactions between the Li metal electrode and dissolved polysulfides (L₂S_n or PS) which appear as reaction intermediates in the cathode.^[5] This phenomenon generates a low Coulombic efficiency (CE), fast capacity decay and a high self-discharge rate, especially at high states of charge (SoC), detrimental for the efficiency and stability of the system.^[6,7] Lithium dendrite growth, in turn, causes safety concerns and likewise gives rise to poor CE and loss of active lithium. While most of the research on Li–S batteries has focused on the sulfur positive electrode, the perhaps equally important Li metal negative electrode has received disproportionately little attention.^[4]

For example, the development of the morphology of the Li metal anode, the chemical composition of the solid electrolyte interphase (SEI) layer formed on it, and the interplay between these phenomena, are far from well understood. It has been suggested that application of pressure between the electrodes lowers the roughness of the lithium anode^[8] and that a reduced surface roughness lead to a longer cycle life.^[9,10] As the dendritic morphology is largely correlated to a high specific surface area, which acts as a “substrate” for SEI formation, the low stability SEI layers can crack easily during repeated morphological deformation. This then causes increasing lithium dendrite growth and the formation of “dead lithium” during battery cycling, which will eventually bring large irreversible capacity losses.

In this context, it is important to consider that by far the most common Li–S cells are prepared with a large excess weight of lithium metal relative to the positive sulfur electrode. A lithium metal foil with a conventional thickness of 125 µm corresponds to approximately 20 times in excess of lithium compared with practical sulfur-loadings (2–2.5 mg_s cm⁻² electrode). The large thickness of the lithium metal electrode adds ‘dead’ weight and volume into the cell, thereby decreasing

[a] Dr. M.-T. Lee, Dr. H. Liu, Prof. D. Brandell
Department of Chemistry – Ångström Laboratory
Uppsala University
Uppsala University, Box 538, 75121, Uppsala, Sweden
E-mail: daniel.brandell@kemi.uu.se
ming-tao.lee@kemi.uu.se

 Supporting information for this article is available on the WWW under
<https://doi.org/10.1002/batt.202000145>

 An invited contribution to a Special Collection on Lithium Metal Anode Processing and Interface Engineering.

 © 2020 The Authors. Published by Wiley-VCH GmbH. This is an open access article under the terms of the Creative Commons Attribution License, which permits use, distribution and reproduction in any medium, provided the original work is properly cited.

energy density and increasing materials costs. From an industrial perspective, it is therefore crucial to implement a very thin ($< 50 \mu\text{m}$) lithium metal foil.

In scientific literature, a few attempts have been made employing and analysing thin Li metal foils.^[11–13] When comparing thick and thin Li metal foils, Jeschull et al.^[11] and Chen et al.^[13] discovered more rapid capacity decay for the thin metal foil, which indicated that such a limitation on the Li metal anode induces earlier capacity fade. This was explained by the poor efficiency of the Li metal electrode, which requires a high loading for a well-behaved surface morphology. Not specifically in the context of Li–S batteries, Shi et al.^[12] studied the application of a thin Li metal anode (50 μm in thickness) in Li|Li pouch cells, and then discovered that the failure mechanisms were dependent on the applied current density. At low current densities, the proposed failure mechanism was correlated to formation of “dead” Li and SEI layer growth, while for higher current densities sharp dendrites generated short-circuits. Recently, Chen et al. showed that through tailoring of the electrolyte system, some of the more dramatic consequences of employing a thin Li metal anode in Li–S batteries could be mitigated.^[13] By employment of a mixed diisopropyl ether (DIPE)-based electrolyte with sulfurized polyacrylonitrile (SPAN) cathodes, the better performance could be ascribed by a more compact morphology, lower interfacial resistance, and a more stable SEI.

The electrode surface chemistry is crucial for the stability and performance of Li-based batteries through the formation of SEI layers. This has been known for a long time, and the Li–S battery constitutes no exception. Recently, there have been considerable efforts made on understanding the surface chemistry of Li metal electrodes in Li–S batteries using X-ray photoelectron spectroscopy (XPS).^[14,15] Aurbach et al.^[15] showed how LiNO₃ as an electrolyte additive contributes positively by preventing the redox shuttle mechanism. Xiong et al.^[14] further demonstrated the structure of the SEI multilayers on Li metal electrodes in Li–S cells by depth profiling XPS.

However, while being important contributions, these studies have utilized thick Li metal foil. It is still unknown how the surface chemistry is affected by employing an ultrathin Li metal electrode – yet this is likely realistic for cell balancing of commercial Li–S cells. Considering the difference in electrochemical performance between thick and thin Li metal foils, it can be expected that a corresponding difference exists in the surface chemistry, which is in a dynamic interplay with different ageing and failure mechanisms in Li–S cells.

In this work, we therefore take a step towards understanding the surface chemistry of Li metal electrodes which are only 30 μm thick. These are employed versus an optimized positive electrode that delivers a high reversible capacity ($\sim 900 \text{ mAh g}^{-1}$) at a decent sulfur-loading (2–2.5 mg S cm^{-2}), using an optimized electrolyte (6 μL per 1 mg of S) composed of lithium (trifluoromethanesulfonyl)imide (LiTFSI) and LiNO₃ co-salt in a mixture of 1,3-dioxolane (DOL) and 1,2-dimethoxyethane (DME) ($v/v = 1:1$). XPS was used as the main characterisation tool for this work, since it provides unique surface and chemical sensitivity, and has been widely employed for studies of SEI

layers.^[16–19] As a complementary method, electron microscopy was used to study the morphological behaviour of the Li metal electrode and correlated to the XPS results.

2. Results and Discussion

Coin cells, with either a thick (125 μm) or a thin (30 μm) Li metal foil were assembled as described in the experimental section and cycled at a constant current of 0.1 C. The discharge capacity (Q_d) and C.E. of these cells are shown in Figure 1. The cell with the thin Li metal electrode exhibits a C.E. of ca. 95% until the 40th cycle, where the C.E. starts to drop significantly. It is merely ~80% around the 70th cycle, and then decays continuously with a rate of ca. 1 percentage point per cycle. By comparison, only a 0.25 percentage-point decrease in C.E. per cycle was observed for the thick Li metal electrode cell after cycle 80, and it was still above 90% after 89 cycles. A low C.E. indicates that side reactions are occurring between Li and the electrolyte, and a decreasing C.E. indicates that these processes are accelerating. As seen in Figure 1, both cells could maintain a stable specific capacity of ca. 900 mAh g^{-1} and a C.E. of >90% until about the 50th cycle, while the thin Li metal electrode cell actually displayed a somewhat higher capacity. Both cells experienced a decrease in discharge capacity during this period, most likely due to electrolyte decomposition, which reduces sulfur utilization and ultimately causes a large increase in internal resistance, as has previously been observed.^[21] After 60–70 cycles, however, the capacity starts to fall comparatively

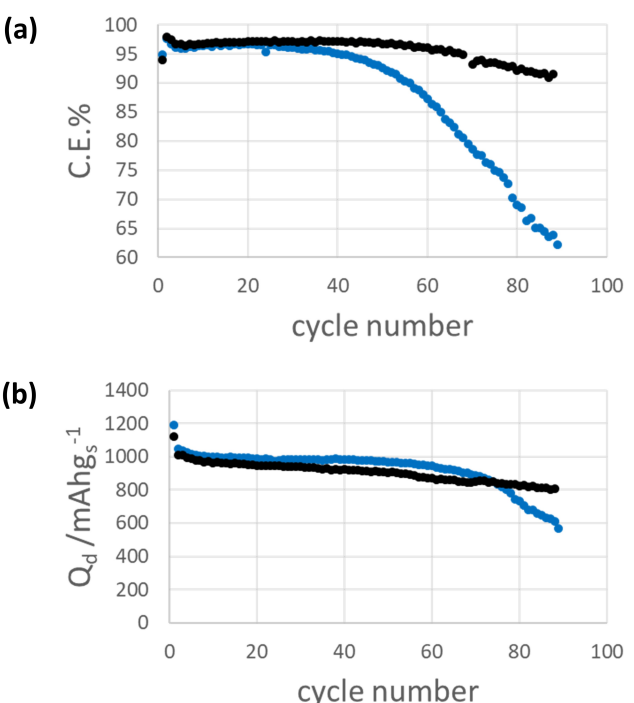


Figure 1. Coulombic efficiency (C.E.%; a) and specific discharge capacity (Q_d ; b) of Li–S cells with 30 μm (blue symbols) and with 125 μm (black symbols) Li metal electrode under galvanostatic cycling at 0.1 C (167.2 mA g^{-1}).

rapidly for the cell with thin Li metal foil. One reason for this could be the lithium morphology development, associated with the difference in experienced pressure on the Li metal electrode. A thick Li metal foil should generate a larger and more uniform mechanical pressure in the cell than a thinner foil in the same coin cell configuration, due to that the thin foil is mechanically unstable. It is indeed very flexible and easily wrinkled, and a lower degree of roughening of the lithium surface during cycling of thick Li anodes can be anticipated.^[9] The reduction in the surface roughness of Li surface then allows for subsequent capacity fading mechanisms to set in at a later stage, thereby leading to a longer lifespan of the cell. At the point of opening the cells, after the 89th cycle, the capacity difference was approximately 200 mAh g_s⁻¹ between the cells.

Comparisons of the surface morphology of the Li electrodes are shown in Figure 2. The surface of the pristine foils shows very little differences, and the pristine Li foils are free from any depositions on the surfaces (Figure 2a and b). After 1 cycle (including a formation cycle), a more compact Li deposition can be seen on the thick Li electrode (Figure 2d) surface than on the thin Li electrode (Figure 2c), where it generates a more porous structure. This could be attributed to the higher mechanical pressure in the cell with the thicker Li foil. This also suggests that there is a higher surface area in the cell with the thin Li foil, and the surface morphology is generally considerably less homogeneous (see Figure 1). The increasing roughness of lithium within a small number of cycles has also been seen by Lacey et al.^[5] The reason for this is likely a much more non-uniform current distribution on the thinner anode, and the

large extent of the redox shuttle current in the first five cycles.^[5]

Figure 2e shows the surface morphology of thin Li electrodes from the Li-S cells kept at OCV for about ~3 days (inset) and ~47 days before opening. The surface of the ~3 days rest (i.e., the time equal to 1 full cycle including a formation cycle) Li electrode is very similar to the pristine Li foil, while after very long resting time, the surface morphology has changed completely. The morphology of the surface layer after a long rest time is strikingly different when compared to the Li electrodes cycled for only one cycle (Figure 2c). For the ~47 days rest battery (at long OCV conditions), the structure appears to have a mossy texture. This is interesting, since no electrochemical driving force was applied on the system, but yet it undergoes extensive ageing. The likely origin for this is that dissolved PS in the electrolyte corrode the surface of lithium anode and form Li₂S_x ($x > 1$). These precipitated species have previously been suggested to be composed of short chain PS such as Li₂S₂ and Li₂S₃, with additional components from oxidized sulfur species (e.g. Li₂SO₃), formed by reactions with LiNO₃.^[5] This is also supported by the following XPS results.

SEM images of the thin Li metal electrode after 89 cycles are shown in Figure 2f. The small photo inset displays the thin Li electrode on a stainless-steel spacer (original colour: silver). In the center part (darker brown colour), a lithium depleted zone is seen, where only a few lithium dendrites can be observed with SEM (left half). The right half of the SEM image in Figure 2f corresponds to the lighter brown colour area in the inset photo, and illustrates very densely deposited Li with no obvious globular structures. The origin of the two zones of the thin Li metal is due to the mismatch in diameter between the Li metal foil discs and the sulfur composites electrodes. Thereby, the effectively cycled zone is in the center where two electrodes overlap, and where the current density is high. Bulk Li in this center zone is therefore gradually consumed, correlated to the generation of "dead" Li during the continuous plating/stripping process. This consumption is more severe in the center than at the edges, and it will progressively take place until the Li excess in the cell is gone. In this case, the cell capacity will not be limited only by the composites sulfur electrode.

To further investigate the surface composition of these Li electrodes, XPS spectra were collected from the same samples as examined by SEM. Discussion of C 1s and Li 1s peaks can be found in the supporting information. In the following, we primarily focus on the S 2p spectra. In Figure 3, the sulfur 2p XPS spectra of the thin Li metal electrode samples are shown. As can be seen, the spectra display several peaks, which can be attributed to different S-containing species according to XPS peak assignments described previously.^[20] The oxidized sulfur species (OSS) appear at peak 1 at ~169 eV, which is assigned to both sulfate ([SO₄]²⁻, S(+VI)) and the sulfone group (R-SO₂-R) of the TFSI anion. OSS also appear at peak 2, at ~167 eV, which correspond to sulfite ([SO₃]²⁻). Reduced sulfur species (RSS) can instead be observed in the deconvolution of S 2p spectra under the broad sulfide region (binding energy around 165–160 eV), consisting of three components: peak 3 which corresponds to

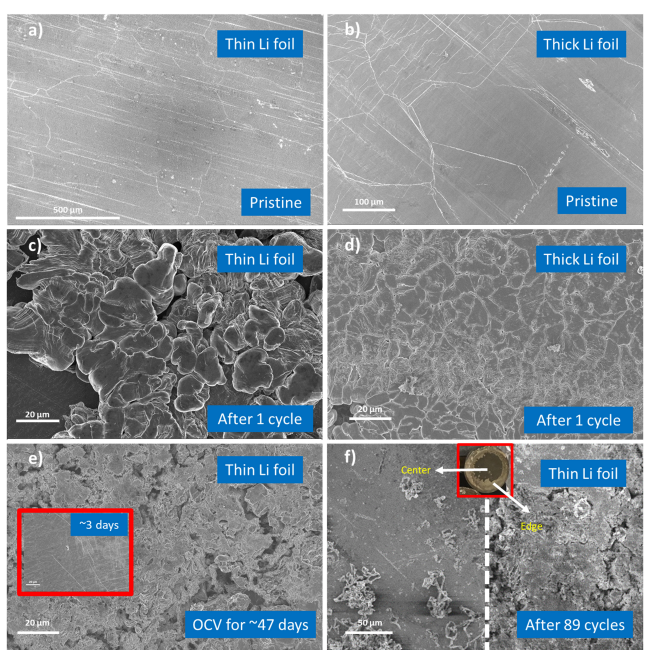


Figure 2. SEM micrographs of the surface of Li metal electrodes in the Li-S cells. a) 30 μ m pristine Li metal foil, b) 125 μ m pristine Li metal foil, c) 30 μ m Li metal electrode after 1 cycle (charged state), d) 125 μ m Li metal electrode after 1 cycle (charged state), e) 30 μ m Li metal electrode at OCV, self-discharged for ca. 47 days (inset: for ~3 days), f) 30 μ m Li metal electrode after 89 cycles (charged state).

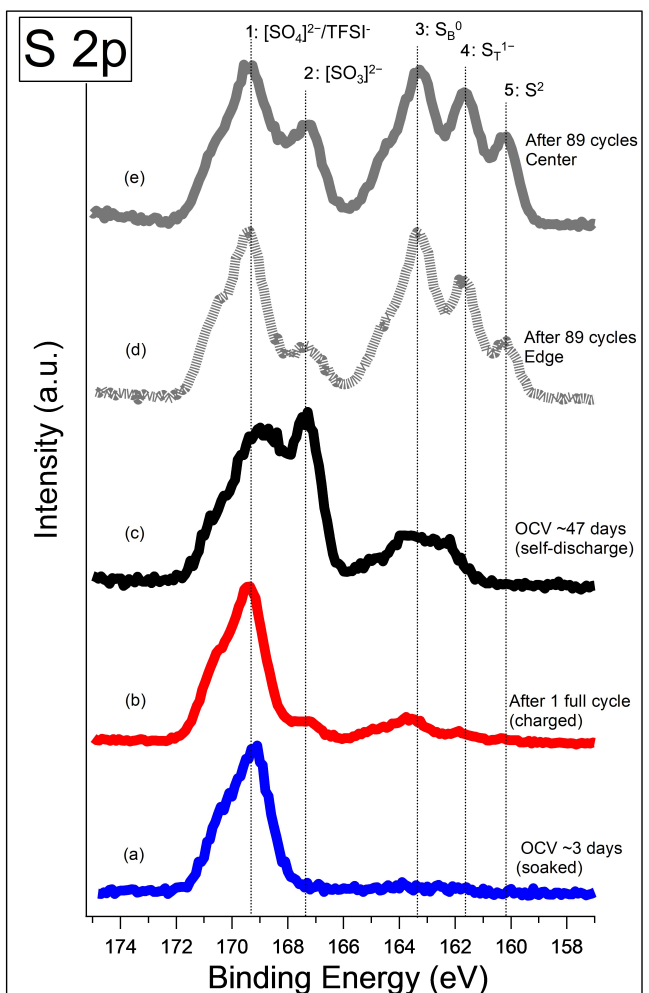


Figure 3. Sulfur 2p XPS spectra of thin Li metal electrodes.

bridging sulfur (S_B^0) of the lithium polysulfides, peak 4 which is terminal sulfur (S_T1^-) and peak 5 which is the sulfide anion (S^{2-}) of Li_2S , respectively. Note that all spectra are normalized to have the same intensity as peak 1. The deconvoluted XPS spectra of S 2p peaks are summarized in Table S1.

Figure 3a (the blue line) represents the sample when the thin Li anode is left to rest at OCV conditions for a time equal to 1 full cycle (~3 days) in the Li–S battery. Only one prominent peak at 169.2 eV appear, which can be attributed to sulfates. These originate from the reaction product between dissolved PS molecules with the lithium metal in the presence of $LiNO_3$, and minor residuals from the TFSI anion. When instead applying current to the cell (after a single full cycle with immediate extraction from the cell; the red line in Figure 3b), the $LiNO_3$ containing electrolyte is rapidly reduced at the Li surface to form a passivating layer on the surface. This is seen as the sulfite (SO_3 in Li_2SO_3 ; peak 2) starts to appear for this sample. Moreover, the three peaks at lower binding energy (i.e. peak 3, 4, and 5) corresponding to Li_2S_x are also becoming visible. These species are formed by the electrochemical processes in the Li–S cell, and it is seen that they rapidly migrate over to the anode side where they are deposited. It is

also important to note that there is a signal from the final reaction product Li_2S at ~160 eV, which is often found in the inner parts of the SEI layer in Li–S cells.^[5,14,15]

After about 47 days exposure to the electrolyte at OCV conditions (Figure 3c; black line), and as compared to the more briefly exposed samples in Figure 3 a and b, there is a striking build-up of contributions from OSS. It should be pointed out that the dominant product is Li_2SO_3 (peak 2).^[15] There are no Li_2S species (peak 5) detected on this surface, which could be due to that this reaction product is not formed during self-discharge conditions. However, there exist contributions from the other two reduced sulfur species, i.e., peak 3 at ~164 eV and peak 4 at ~162 eV, which have quite pronounced relative intensities.

After 89 cycles, the XPS spectra (Figure 3d and e) display all five different sulfur environments. Compared to the Li anode after 1 cycle or after self-discharge, the amount of RSS has increased significantly. This increase in the RSS at higher cycle numbers, and the inverse proportionality between RSS and CE, could also be observed in tests performed under similar conditions but utilizing a thick Li foil (see Figure S1). In correlation to the formation of RSS on the Li anode, a more unstable SEI is observed which corresponds to enhanced parasitic redox reactions between Li and the polysulfides.^[5] This explains the gradual decrease in CE.

The fractions of OSS and RSS from the S 2p XPS spectra in Figure 3 are shown in Figure 4a for all samples. Moreover, the normalized salt degradation species (SDS), i.e. the sum of RSS found in S 2p, Li_3N in N 1s (Figure S2a) and LiF in F 1s (Figure S2b) XPS spectra, are shown in Figure 4b. Note that in Fig 4b, the value of the peak corresponding to SDS for the “soaked” sample is set to unity, while all integrated areas corresponding to different core levels are normalized to the corresponding sensitivity factor. Thereby, the integrated peak areas can be translated into fraction of atomic concentrations.

As discussed above, the RSS fraction (Figure 4a) is increasing with both cycle number and the time the Li metal anode has been in contact with the electrolyte in the cell assembly. No RSS were detected in the merely soaked sample. After 1 cycle, the RSS are about 15% of the entire S 2 p environments, and increase to around 20% in the self-discharged sample (Figure 3c). After 89 cycles, the amount of RSS has become >50% of all sulfur species observed in the S 2p spectra, both in the center and at the edge zones. There is only a very small amount of LiF contributing to the SDS on the Li anode that has been exposed to the electrolyte for about 3 days.

Presumably, this is coming from some degradation of the LiTFSI salt in the electrolyte, which rapidly gets deposited at the Li surface. After 1 single cycle, the total amount of SDS on the surface have increased four times relative to the merely soaked sample. For the cycled sample (after 1 cycle), RSS, LiF , and Li_3N are contributing fairly equally to the total SDS. This means that LiTFSI is decomposing to some degree already during the initial cycles. Interestingly, after a long period at rest conditions (i.e., ~47 days), the SDS have increased 10 times relative to the soaked sample. It is worth mentioning that the SDS on this electrode sample comprise RSS and LiF , but that

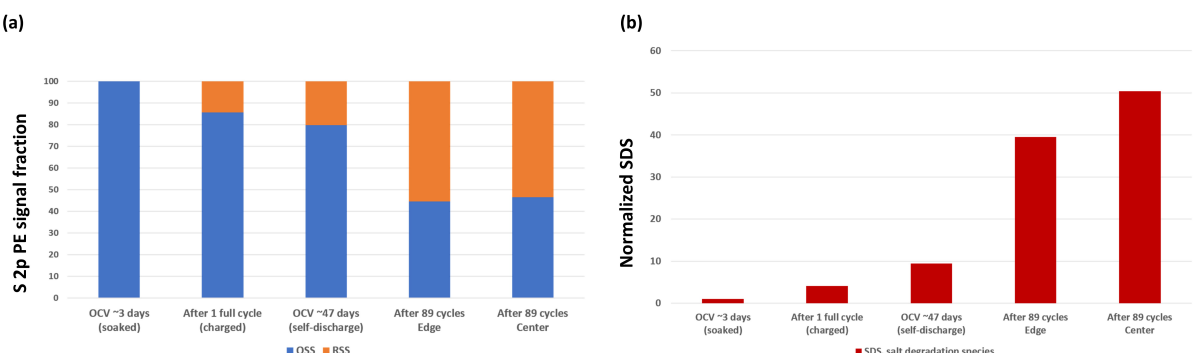


Figure 4. a) Fraction of integrated S 2p peak area for OSS (blue bar; sum of peak 1 and 2 in Figure 3) and RSS (orange bar; sum of peak 3, 4 and 5 in Figure 3) of the investigated Li metal electrodes, summarized from the S 2p PE spectra in Figure 3. b) Normalized atomic fraction of salt degradation species (SDS) on the thin Li metal electrodes. SDS = RSS + Li₃N + LiF

there is a negligible amount of Li₃N. After 89 cycles, there is a more than 40 times increase in SDS species as compared to the soaked sample (~3 days), dominated by RSS, as observed in XPS spectra from the sample center region (50 times) and at the edge regions of the Li metal disc. This indicates that the majority of the lost capacity (as observed in Figure 1b) is due to the polysulfide shuttle rather than losses originating from electrolyte decomposition.

Figure 5 shows the spectroscopic comparisons of the sulfur surface species on thin and thick Li metal anodes after 89 cycles. For the thick Li electrode, peak 2 that is corresponding to Li₂SO₃ displays a significantly lower fraction, with peak 4 (Li₂S₂) and 5 (Li₂S) being rather pronounced, when compared to the thin Li metal anode after 89 cycles. Thus, there appears to be a reverse correlation between the formation of RSS (peak 4 and 5) and OSS (peak 2). This observation can be explained by a gradient in oxidation states of the surface species, where species with the lowest oxidation state (e.g. Li₂S₂ and Li₂S) are formed closer to the Li metal surface, whereas species closer to the electrolyte side appear with higher oxidation states (e.g., species S=O bonds).^[14,15] Therefore, the relatively larger XPS signals within the probe volume (a few nm in depth) from Li₂S₂ and Li₂S for the thick Li anode suggest a comparatively thinner layer of higher oxidation state species (also seen in the O 1s spectra in Figure S5), which in turn obscures the signals from the RSS compounds to a lesser degree. Consequently, for the thin Li metal anodes after 89 cycles, there are stronger Li₂SO₃ XPS signals, which then obscures the peaks corresponding to Li₂S₂ and Li₂S.

The observation that (see Figure 5), after cycling, there is a build-up of more Li₂SO₃ species on the surface of the thin Li anode than the thick Li is intriguing. It has been discussed that Li₂SO₃ is the final product of reduced species from LiNO₃ and TFSI.^[15] The higher concentration of this reaction product suggests a more extensive consumption of LiNO₃, which has a lower concentration than LiTFSI and therefore should be the limiting reactant. This more extensive reaction could well be due to the rougher surface of the thin Li anode, which provides more surface area for SEI formation in each cycle. Therefore, the Li passivation due to LiNO₃ is less effective for this

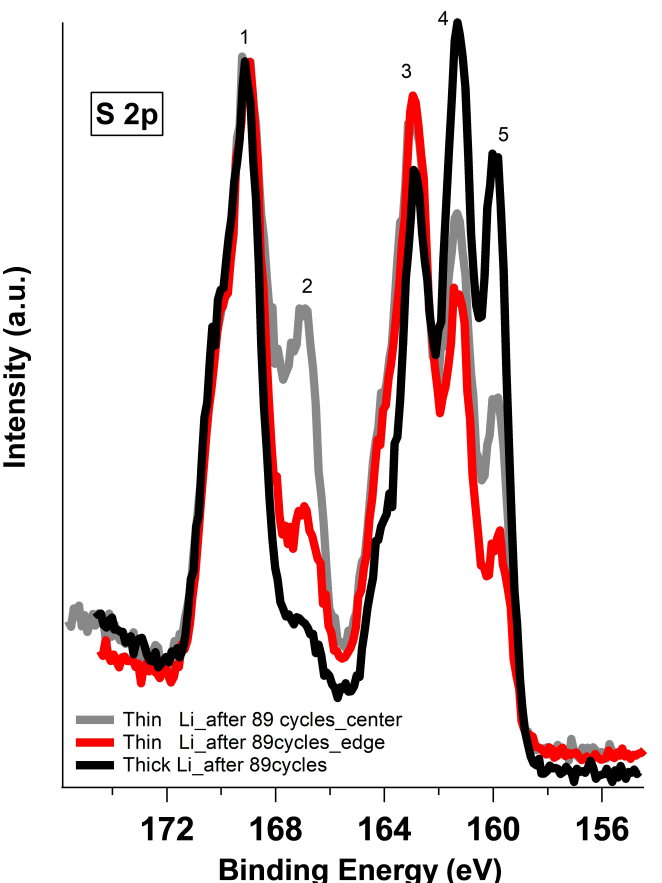


Figure 5. S 2p XPS spectra of the investigated thin vs. thick Li metal electrodes after 89 cycles. Grey curve: center part of thin Li metal electrode (the same spectrum as in Figure 3e). Red curve: edge part of the same sample (the same spectrum as in Figure 3d). Black curve: thick Li metal electrode. Note that all spectra are normalized to have the same intensity as peak 1.

electrode, since small amounts of LiNO₃ are consumed in each cycle. Thereby, the nitrate co-salt cannot provide such a positive effect in preventing the shuttle effect in Li–S cells when the Li-anode is very thin.^[22]

3. Conclusions

To understand the role of the surface chemistry in Li–S cells, thin Li metal electrodes were investigated using a combination of electrochemical measurements, XPS and SEM. The results indicate that the electrochemical performance in these Li–S cells utilizing a 1 M LiTFSI in DOL:DME electrolyte solution with 0.25 M LiNO₃ additive is correlated to surface morphology, chemistry and SEI layer formation. While the general chemical composition and morphology of the SEI films for both thick and thin Li metal anodes were consistent with previous studies,^[14,15] the cause of earlier cell fading of the thin Li metal electrode could be partly attributed to a rougher Li metal electrode. As seen from the XPS analyses, this changes the SEI composition and indicates a significantly higher consumption of the LiNO₃ additive as compared to a thick Li metal anode, and hence shortens the cycle life. Interestingly, the enrichment of oxidized sulfur species, i.e. Li₂SO₃ on the thin Li anode, which is correlated to consumption of LiNO₃, was also found on the surface of the thin Li anode after self-discharging conditions. This indicates that the consumption of LiNO₃ is continuous also during rest, which can significantly influence the Li–S battery shelf life. These results indicate that if employing a thin Li metal electrode to achieve a good cell balancing, a stabilization of the anode surface in Li–S cells becomes even more critical than for cells using a large excess of Li foil.

Experimental Section

Materials

Li–S cell preparation. All sulfur-based cells were prepared in CR2025-format coin cells (Hohsen). Coin cells were constructed with 15 mm diameter Li metal foil discs as the negative electrodes and 13 mm discs of sulfur composites as the positive electrode. The thickness of the lithium foil was 30 µm (“thin lithium foil”, Rockwood Lithium) or 125 µm (“thick lithium foil”), respectively. Experimental details of making the composite electrode have been described in a previous study.^[20] S was manually mixed with Ketjenblack (KB) in a mortar in a 65:21 mass ratio and heated to 155 °C for 20 minutes. The mixture was then blended with Super C65, carbon nanofibers (CNF), poly(ethylene oxide) (PEO) and poly(vinylpyrrolidone) (PVP) for a target electrode composition of 65% S, 21% KB, 3.5% C65, 3.5% CNF, 5.6% PEO, 1.4% PVP (in weight). The overall S:C ratio in the positive electrode was 2.23:1 (65:28). A circular Celgard separator (diameter 17 mm) was put between the positive and negative electrode. Electrolyte of 1 M lithium bis(trifluoromethanesulfonyl)imide (LiTFSI) and 0.25 M lithium nitrate (LiNO₃) in a mixture of 1,3-dioxolane (DOL) and 1,2-dimethoxyethane (DME) (v/v = 1:1) with a fixed volume of 6 µL mg_S⁻¹ was applied to the cells.

Electrochemical characterization

All electrochemical tests were conducted using an Arbin BT-2043 battery testing system. Assembled cells were first rested for 6 hours and then subjected to a formation cycle by discharging at a rate of 0.02 C to 1.9 V and then charged at 0.04 C to 2.6 V. The cells were then cycled at 0.1 C between 1.8 and 2.6 V. The C-rate was determined from theoretical capacity of sulfur (1672 mAh g_S⁻¹, i.e.,

C = 1672 mA g_S⁻¹) and the mass of sulfur in the electrode (g_S). Each discharge-charge cycle was limited to a maximum time of 10 h (i.e., the theoretical capacity).

Surface characterizations of Li metal

SEM and XPS analyses. Coin cells were made with the same procedure described above for post-mortem SEM and XPS analyses. These cells went through the same formation cycle as previously described, and then two additional cycles at 0.1 C. Thereafter, the electrodes were separated from the cells in the fully charged state. Li electrodes were rinsed with 1–2 ml of DME:DOL (1:1).

SEM micrographs were obtained using a Merlin, Carl Zeiss instrument. XPS spectra were acquired with a PHI 5500 spectrometer (Physical Electronics) using monochromatic Al K α radiation (1486.7 eV). The chamber pressure was maintained at $\leq 1 \times 10^{-8}$ Torr during all measurements. XPS data were analysed using the Igor Pro 6.37 software assuming Gaussian/Lorentzian (10–30% Lorentzian) line shapes and utilizing Shirley background subtraction. All sulfur lines were curve fitted using a doublet peak with a spin-orbit splitting of 1.18 eV and an intensity ratio of 2:1, characteristic for S 2p.

Acknowledgements

The authors are grateful to Swedish Energy Agency for the financial support through STARC (42762-1), the LIBchallenge project, and the Swedish strategic research programme StandUp for Energy.

Conflict of Interest

The authors declare no conflict of interest.

Keywords: Li–S battery • Li metal electrode • thin metal foil • surface chemistry • X-ray photoelectron spectroscopy

- [1] Oxis Energy, Retrieved from <https://oxisenergy.com>.
- [2] Sion Power, Retrieved from <https://sionpower.com>.
- [3] Y. V. Mikhaylik, J. R. Akridge, *J. Electrochem. Soc.* **2004**, *151*, A1969–A1976.
- [4] X.-B. Cheng, J.-Q. Huang, Q. Zhang, *J. Electrochem. Soc.* **2018**, *165*, A6058–A6072.
- [5] M. J. Lacey, A. Yalamanchili, J. Maibach, C. Tengstedt, K. Edström, D. Brandell, *RSC Adv.* **2016**, *6*, 3632–3641.
- [6] X. Fan, W. Sun, F. Meng, A. Xing, J. Liu, *Green Energy Environ.* **2018**, *3*, 2–19.
- [7] G. Ma, Z. Wen, M. Wu, C. Shen, Q. Wang, J. Jin, X. Wu, *Chem. Commun.* **2014**, *50*, 14209–14212.
- [8] T. Hirai, *J. Electrochem. Soc.* **1994**, *141*, 611–614.
- [9] Y. Mikhaylik, I. Kovalev, R. Schock, K. Kumaresan, J. Xu, J. Affinito, *ECS Trans.* **2009**, *25*, 23–34.
- [10] P. P. Natsiavas, K. Weinberg, D. Rosato, M. Ortiz, *J. Mech. Phys. Solids.* **2016**, *95*, 92–111.
- [11] F. Jeschull, D. Brandell, K. Edström, M. J. Lacey, *Chem. Commun.* **2015**, *51*, 17100–17103.
- [12] P. Shi, X. Cheng, T. Li, R. Zhang, H. Liu, C. Yan, X. Zhang, J. Huang, Q. Zhang, *Adv. Mater.* **2019**, *31*, 1902785.
- [13] W. Chen, C. Zhao, B. Li, Q. Jin, X. Zhang, T. Yuan, X. Zhang, Z. Jin, S. Kaskel, Q. Zhang, *Energy Environ. Mater.* **2020**, *3*, 160–165.
- [14] S. Xiong, K. Xie, Y. Diao, X. Hong, *J. Power Sources* **2014**, *246*, 840–845.

- [15] D. Aurbach, E. Pollak, R. Elazari, G. Salitra, C. Scordilis Kelley, J. Affinito, *J. Electrochem. Soc.* **2009**, *156*, 694–702.
- [16] E. Peled, S. Menkin, *J. Electrochem. Soc.* **2017**, *164*, A1703–A1719.
- [17] P. Verma, P. Maire, P. Novák, *Electrochim. Acta* **2010**, *55*, 6332–6341.
- [18] J. Maibach, F. Lindgren, H. Eriksson, K. Edström, M. Hahlin, *J. Phys. Chem. Lett.* **2016**, *7*, 1775–1780.
- [19] A. M. Andersson, A. Henningson, H. Siegbahn, U. Jansson, K. Edström, *J. Power Sources* **2003**, *119*–*121*, 522–527.
- [20] Y.-C. Chien, R. Pan, M.-T. Lee, L. Nyholm, D. Brandell, M. Lacey, *J. Electrochem. Soc.* **2019**, *166*, A3235–A3241.
- [21] M. J. Lacey, K. Edström, D. Brandell, *Chem. Commun.* **2015**, *51*, 16502–16505.
- [22] M. Hagen, D. Hanselmann, K. Ahlbrecht, R. Maça, D. Gerber, J. Tübke, *Adv. Energy Mater.* **2015**, *5*, 1401986.

Manuscript received: June 23, 2020
Revised manuscript received: August 7, 2020
Accepted manuscript online: August 11, 2020
Version of record online: September 10, 2020